

Non-metallocene rare earth metal catalysts for the diastereoselective and enantioselective hydroamination of aminoalkenes [☆]

Kai C. Hultsch ^{*}, Denis V. Gribkov, Frank Hampel

Institut für Organische Chemie, Friedrich-Alexander Universität, Erlangen-Nürnberg, Henkestr. 42, D-91054 Erlangen, Germany

Received 29 September 2004; received in revised form 11 November 2004; accepted 11 November 2004

Available online 16 February 2005

Abstract

In this short review we summarize our work on new cyclopentadienyl-free rare earth metal catalysts for the diastereoselective and enantioselective hydroamination of aminoalkenes. Non-metallocene rare earth metal catalysts based on diamidoamine, biphenolate and binaphtholate ligands are readily available through alkane and amine elimination procedures. Diamidoamine yttrium complexes are efficient catalysts for the highly diastereoselective cyclization of 1-methyl-pent-4-enylamine to yield *trans*-2,5-dimethyl-pyrrolidine with *trans* to *cis* ratios of up to 23:1. The X-ray crystal structural analysis of [(2,6-Et₂C₆-H₃NCH₂CH₂)₂NMe)Y{N(SiMe₃)₂}] is reported in which yttrium is coordinated in a highly distorted tetrahedral fashion. 3,3'-Di-*tert*-butyl substituted biphenolate complexes tend to form phenolate-bridged hetero- and homochiral dimers. The low steric demand of the *tert*-butyl substituents resulted also in low enantioselectivities in hydroamination/cyclization reactions. Binaphtholate complexes with sterically more demanding tris(aryl)silyl substituents were more efficient catalysts; giving enantioselectivities of up to 83% ee. These catalysts could also be applied in kinetic resolution of chiral aminoalkenes giving *k*_{rel} values as high as 16. Catalyst activities strongly depend on the reactivity of the leaving group which is protolytically exchanged for the substrate during the initiation step. Complexes with bis(dimethylsilyl)amido ligand initiate rather sluggishly because of the low basicity of this amido ligand and appreciable catalytic activity is only observed at elevated temperatures. Aryl and Alkyl complexes showed significant better rates comparable in magnitude to lanthanocene catalysts.

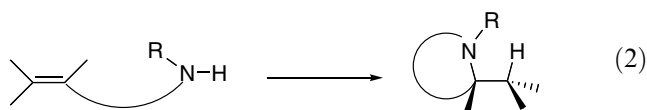
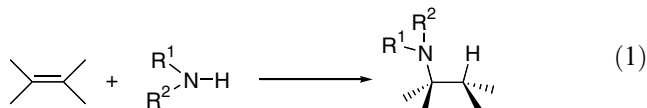
© 2005 Elsevier B.V. All rights reserved.

Keywords: Asymmetric catalysis; Hydroamination; Rare earth metals; Non-metallocene complexes

1. Introduction

The hydroamination is a highly atom economical process in which an amine N–H bond is added to an unsaturated carbon–carbon bond (Eqs. 1 and 2). This reaction is of great potential interest for the waste-free

synthesis of basic and fine chemicals, pharmaceuticals and other industrially relevant building blocks starting from inexpensive precursors [1].



[☆] This paper was first presented at the XIVth International Conference on Homogeneous Catalysis, Munich, July 7, 2004.

^{*} Corresponding author. Fax: +49 9131 852 6865.

E-mail address: hultzsch@chemie.uni-erlangen.de (K.C. Hultsch).

The transition metal catalyzed hydroamination has the significant advantage that stereo- and regiochemistry (e.g., Markovnikov/*anti*-Markovnikov addition) of the hydroamination product may be controlled by tuning the steric and electronic properties of the ligand framework. In particular the generation of new stereogenic centers during the hydroamination process constitutes an attractive application of this reaction, but the development of chiral catalysts for the asymmetric hydroamination of alkenes (AHA) has remained challenging [2].

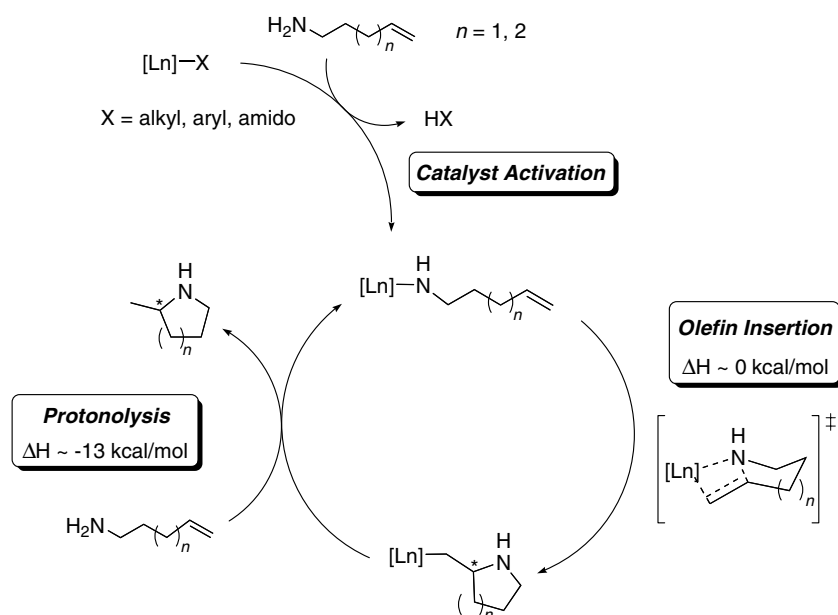
Over the past two decades catalyst systems based on early (groups 3–5, as well as lanthanides and actinides) [1h,1i,1j,1k,3] and late (groups 8–10) [1g,4] transition metals have been developed [5]. Unfortunately, most systems suffer from restrictions in the choice of substrates. Commonly only alkynes, activated alkenes (e.g., alkenes with electron withdrawing groups attached, vinyl arenes, 1,3-dienes or ring-strained alkenes) and certain types of amines (e.g., anilines) react. Marks and coworkers on the other hand have pioneered catalyst systems based on rare earth metals that are highly reactive towards simple alkene substrates [1k,6,7], although the number of reports on *intermolecular* rare earth metal catalyzed reactions are limited [8] and most investigations have focused on *intramolecular* hydroamination reactions.

The mechanism of the rare earth metal catalyzed intramolecular hydroamination involves a metal amido species, which is generated in an activation step via protolytic exchange of an alkyl or amido ligand in the precatalyst by the aminoalkene substrate (Scheme 1) [6,9]. In the first step of the catalytic cycle the alkene inserts into the metal amido bond through a seven-membered chair-

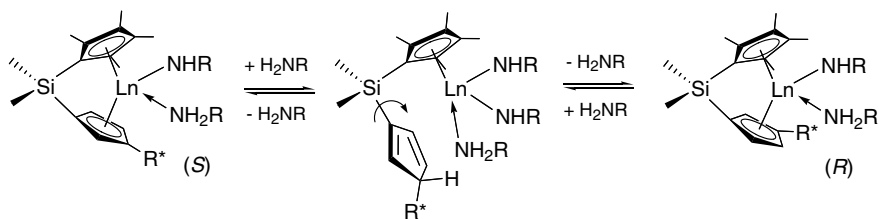
like transition state (for $n = 1$). This step is approximately thermoneutral [9] and it is usually also the rate determining step, giving rise to a zero order rate dependence on substrate concentration and first order rate dependence on catalyst concentration. The resulting rare earth metal alkyl species undergoes fast protonolysis with a second amine molecule, regenerating the rare earth metal amido species and releasing the heterocyclic product.

The first asymmetric hydroamination catalysts based on chiral rare earth metal amido complexes were reported by Marks and coworkers in 1992 [10]. Unfortunately, these C_1 -symmetric chiral *ansa*-lanthanocenes underwent facile epimerization under the conditions of catalytic hydroamination via reversible protolytic cleavage of the metal cyclopentadienyl bond (Scheme 2) [10–12]. Obviously, such an epimerization process is highly unfavourable for efficient asymmetric catalysis. In fact, the enantiomeric excess and absolute configuration of the hydroamination product was independent of the diastereomeric purity of the chiral lanthanocene precatalyst employed [10c]. Furthermore, enantiomeric excess of hydroamination products obtained with these catalysts was limited below 75% ee.

A configurationally stable catalyst seemed to us a *sine qua non* for efficient asymmetric catalysis. We therefore decided to develop hydroamination catalyst systems based on non-cyclopentadienyl ligand sets [13], which should have comparable catalytic activity to the lanthanocene systems, but should not epimerize under the reaction conditions of catalytic hydroamination. A second advantage of non-cyclopentadienyl ligands would be that chiral ligands are usually more easily accessible and can be readily modified [14].



Scheme 1. Simplified mechanism for rare earth metal catalyzed hydroamination/cyclization.



Scheme 2. Epimerization of chiral lanthanocene complexes during the hydroamination reaction ($R^* = (-)$ -menthyl, $(-)$ -phenylmenthyl, $(+)$ -neomenthyl) [10,12].

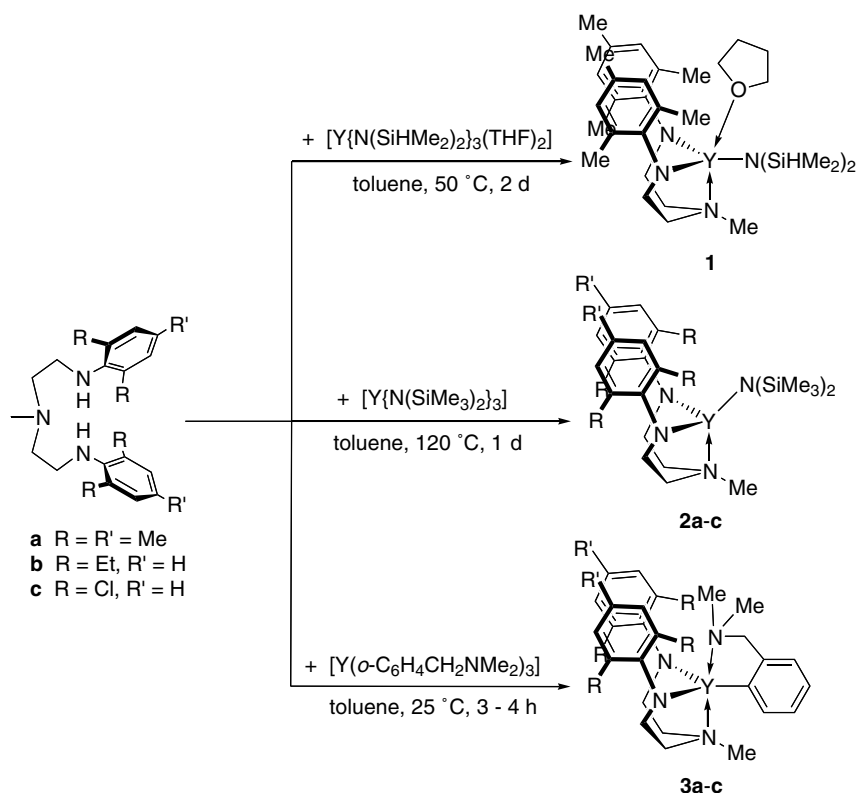
When we began our studies in 2001, the number of non-metallocene rare earth metal hydroamination catalyst systems was limited [15]. Since then, however, several reports have appeared on the application of non-metallocene rare earth metal catalysts in diastereoselective [16] and enantioselective [17] hydroamination.

2. Diamidoamine catalysts for diastereoselective hydroamination of aminoalkenes

2.1. Synthesis and structure of diamidoamine complexes

As one of our first non-chiral model systems we chose complexes based on tridentate diamidoamine ligands, which had been successfully applied in group 4 metal liv-

ing α -olefin polymerization catalysis [18]. The complexes could be prepared conveniently in good to excellent yield via amine or arene elimination starting from tris(amido) yttrium or tris(*o*-C₆H₄CH₂NMe₂) yttrium precursors (Scheme 3) [19]. Whereas the bis(dimethylsilyl)amido complex **1** was obtained under mild reaction conditions, the corresponding bis(trimethylsilyl)amido complexes **2** required much harsher reaction conditions because of formation of undesired by-products at lower reaction temperatures. The amido complexes **1** and **2** showed high thermal stability, but aryl complex **3a** decomposed at room temperature ($t_{1/2} \approx 6$ h), probably via C–H activation of the *ortho*-methyl group of the mesityl substituent. Indicative for this assumption was the decreased rate of decomposition for the sterically more demanding ethyl substituted complex **3b** ($t_{1/2} \approx 2.5$ d) and the absence of decomposition in case of the



Scheme 3. Synthesis of diamidoamine complexes via amine or arene elimination.

2,6-dichlorophenyl substituted complex **3c** after 4 d at 25 °C and 1 h at 70 °C.

Complexes **1** and **3b** have distorted trigonal bipyramidal geometries with a diamidoamine ligand adopting a *fac* coordination mode (Figs. 1 and 2) [19]. The structure of four coordinate complex **2b** [20] can be seen as being intermediate between tetrahedral and seesaw geometry (Fig. 3). The geometry of the diamidoamine ligand in **2b** is very similar to that in **1** and **3b**, despite the lower coordination number of yttrium in this complex (Table 1). Furthermore the bond length of yttrium to the diamidoamine ligand are only slightly shorter in **2b** than in **1**, but comparable to those in **3b**. The unsaturation of yttrium is manifested in two short contacts with methyl groups of the bis(trimethylsilyl)amido ligand, suggesting

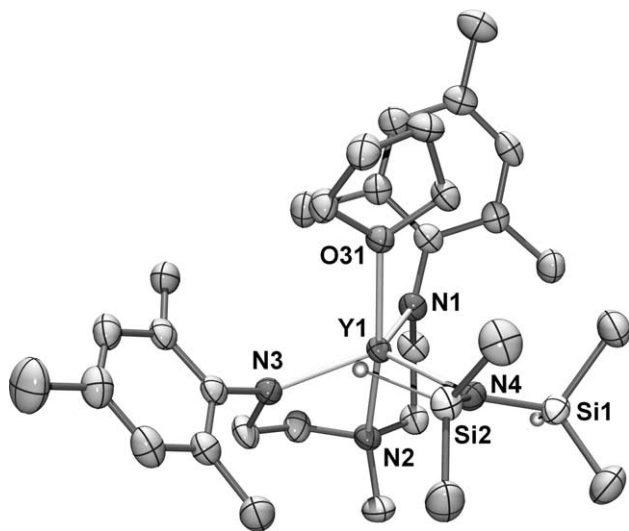


Fig. 1. Structure of five coordinate diamidoamine complex **1**.

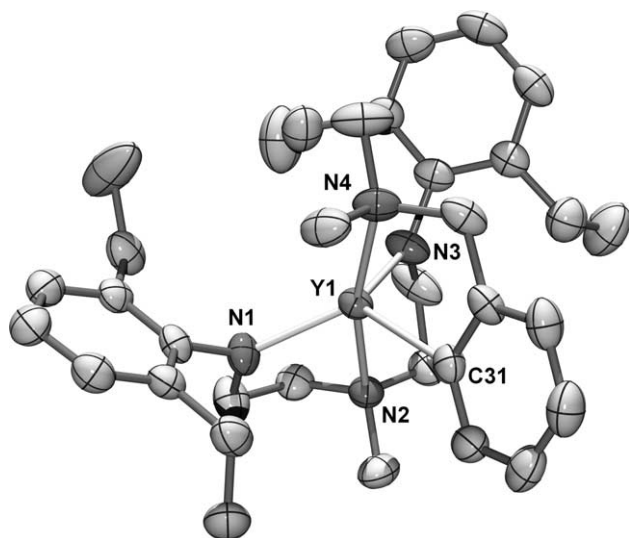


Fig. 2. Structure of five coordinate diamidoamine complex **3b**.

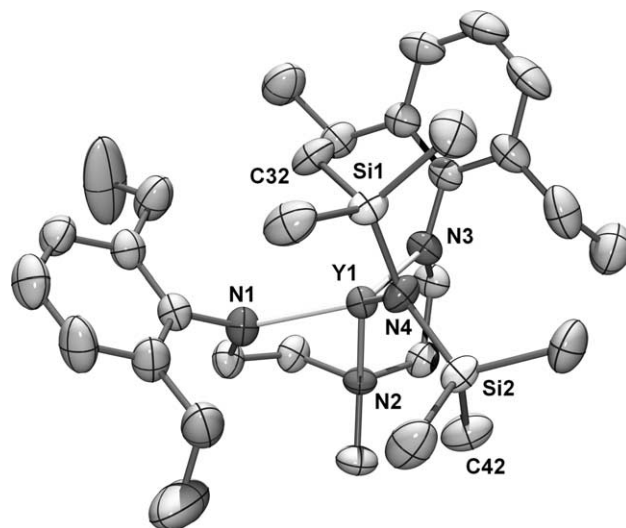


Fig. 3. Structure of four coordinate diamidoamine complex **2b**.

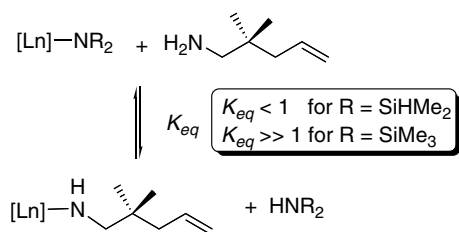
Table 1
Comparison of selected bond lengths (Å), atomic distances (Å) and angles (°) for diamidoamine yttrium complexes **1**, **2b** and **3b**

	1	2b	3b
Y1–N1	2.240(3)	2.223(4)	2.172(4)
Y1–N2	2.480(3)	2.492(3)	2.466(3)
Y1–N3	2.245(3)	2.185(3)	2.219(4)
Y1–N4	2.263(3)	2.233(3)	2.527(3)
Y1...C32		3.019(5)	
Y1...C42		3.064(6)	
Y1...Si1	3.560(1)	3.2657(12)	
Y1...Si2	3.195(1)	3.3101(11)	
N1–Y1–N2	71.08(10)	73.63(14)	73.67(12)
N1–Y1–N3	117.55(10)	117.58(13)	119.51(14)
N2–Y1–N3	72.94(10)	72.37(12)	71.96(12)
N1–Y1–N4	111.98(10)	118.28(14)	118.34(13)
N2–Y1–N4	99.80(9)	144.24(12)	167.48(13)
N3–Y1–N4	123.23(10)	120.04(14)	102.71(12)
Si1–N4–Si2	125.32(16)	134.1(2)	
Y1–N4–Si1	127.31(15)	111.86(17)	
Y1–N4–Si2	106.63(13)	114.08(18)	

the presence of β -SiC agostic interactions similar to previously characterized bis(trimethylsilyl)amido complexes [21].

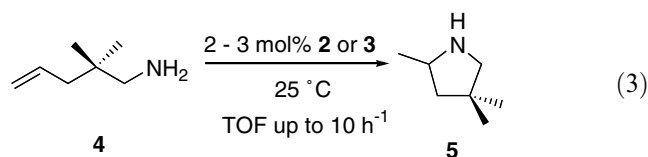
2.2. Catalytic hydroamination/cyclization of aminoalkenes

Complexes **2** and **3** displayed good catalytic activity in the cyclization of aminoalkene **4** at room temperature (TOF 7.6–10 h⁻¹ for **2a,b** and **3a,b**; 1.2 h⁻¹ for **2c** and **3c**, Eq. (3)) which is close to that of homoleptic [Y{N(SiMe₃)₂}]₃ (10 h⁻¹). The bis(dimethylsilyl)amido complex **1** on the other hand showed diminished catalytic activity and required higher reaction temperatures (1.3 h⁻¹ at 40 °C). The catalytic activity of **2a** and **3a**



Scheme 4. Equilibrium of catalyst activation.

was only slightly diminished in the presence of a few equivalents of THF, indicating that the low catalytic activity of **1** is not a result of catalyst deactivation by coordinated THF. In fact, the lower basicity of the bis(dimethylsilyl)amido ligand in comparison to the bis(trimethylsilyl)amido ligand [22] results in an incomplete initiation (Scheme 4) and only a small amount (<20%) of the precatalyst enters the catalytic cycle.



The Thorpe–Ingold-effect [23] favors the cyclization of *gem*-dialkyl substituted **4** in comparison to unsubstituted aminopentene **6**, resulting in a 2- to 10-fold increase in the cyclization rate for most catalyst systems. However, the mesityl substituted complex **3a** showed essentially no activity in the cyclization of **6**, similar to the tris(amido) complex $[Y\{N(SiMe_3)_2\}_3]$ (Table 2). In contrast to that, complex **3c** catalyzed the cyclization of **6** with significant better activity. An explanation for this unexpected difference in reactivity of the two diamidoamine catalysts **3a** and **3c** was uncovered by NMR spectroscopic investigations, which showed that in case of catalyst **3a** the tridentate diamidoamine ligand was protolytically cleaved from the metal by substrate **6**. In case of catalyst **3c** on the other hand, the less basic diamidoamine ligand with electron withdrawing dichlorophenyl substituents remained coordinated to

Table 2
Cyclization of pent-4-enylamine (**6**)

Catalyst	<i>T</i> (°C)	<i>t</i> (h)	Conversion (%)
3a	90	30	4
3c	60	60	97
$[Y\{N(SiMe_3)_2\}_3]$	80	216	6

the metal. However, no ligand dissociation was observed for both catalysts in catalytic reactions of the sterically more demanding *gem*-dimethyl substituted **4**.

Cyclization of 1-methyl-pent-4-enylamine (**8**) leads to *cis*- and *trans*-2,5-dimethyl-pyrrolidine (**9**). Therefore, this substrate was chosen to quantify catalytic activity as well as diastereoselectivity of the catalysts. The preferred formation of the *trans* diastereomer can be explained with minimal 1,3-diaxial interactions in the cyclization transition state (Fig. 4) [6,24]. Simple homoleptic tris(amido) complexes $[Ln\{N(SiMe_3)_2\}_3]$ are inferior catalysts for this particular substrate [15c,16a,19], requiring high reaction temperatures and giving poor diastereoselectivities.

Livinghouse et al. reported the facile cyclization of this substrate under relative mild conditions (60 °C) with high diastereoselectivities (up to 19:1) using a catalyst system generated in situ from $[Ln\{N(SiMe_3)_2\}_3]$ and a vicinal diamine [16]. Unfortunately, information on the nature of the catalytically active species remained limited [25], hampering the elucidation of structure–reactivity/selectivity relationships.

The well-defined diamidoamine complexes **2** and **3** displayed not only good catalytic activity even at room temperature, but also excellent *trans*:*cis* diastereoselectivity of up to 23:1 (Table 3). The sterically least demanding 2,6-dichlorophenyl substituted diamidoamine complexes gave the lowest *trans* to *cis* ratio of 14:1.

Catalysts **2** and **3** were also shown to be reactive towards secondary amines in the bicyclization of aminodiene **10** (Scheme 5), producing 1-aza-bicyclo[2.2.1]heptane derivatives. The first cyclization step generated pyrrolidine **11** with turnover frequencies $>55\text{ h}^{-1}$ at room temperature, but low diastereoselectivities ($\leq 1.4:1$). The second cyclization usually requires heating to 60 °C and the aza-bicyclic product **12** was generated as a mixture of (*endo*:*exo*) and (*exo*:*exo*) isomers (1.4:1 for **2b**). Bicyclization using $[Y\{N(SiMe_3)_2\}_3]$ proceeded faster (4 h, 60 °C, >98% conv.), but afforded an equimolar mixture of the two aza-bicyclic diastereomers.

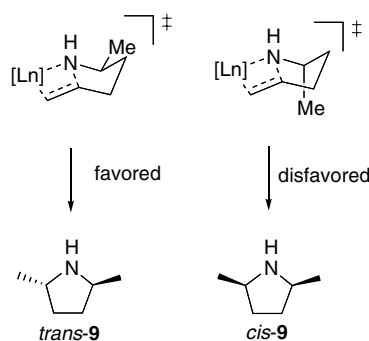
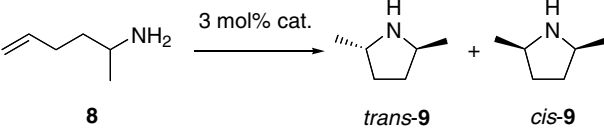
Fig. 4. Plausible cyclization transition states for the preferred formation of *trans*-2,5-dimethyl-pyrrolidine (**9**).

Table 3
Catalytic hydroamination/cyclization of 1-methyl-pent-4-enylamine (**8**)



Catalyst	<i>T</i> (°C)	TOF (h ⁻¹)	d.r.(<i>trans</i> : <i>cis</i>)
2a	25	5.2	22:1
2b	25	6.2	19:1
2c^a	25	9.1	14:1
3a	25	7.8	22:1
3b	25	4.3	23:1
3c	25	6.8	13.5:1
[La{N(SiMe ₃) ₂ }] ₃	90		4:1 ^b

^a 1.6 mol% cat.

^b >99% conv. after 13 h.

3. Biphenolate and binaphtholate catalysts for enantioselective hydroamination of aminoalkenes

3.1. Synthesis of chiral non-metallocene complexes

Our first chiral rare earth metal complexes were based on the biphenolate ligand Biphen²⁻ with stereodirecting *tert*-butyl substituents in 3 and 3' positions (Scheme 6) [26–29]. The monomeric yttrium complex **13** could be prepared via amine elimination in enantiopure and racemic form. However, the *tert*-butyl substituents were not sterically demanding enough to prevent dimer formation. Upon heating of (*rac*)-**13** the phenolate-bridged heterochiral dimer (*R,S*)-**14a** was formed. Furthermore, lanthanum formed exclusively the heterochiral dimer (*R,S*)-**14b** (Fig. 5) because of its larger ionic radius, and an enantiopure complex could not be prepared.

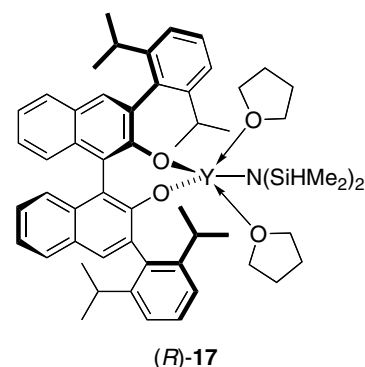
Yet, enantiopure biphenolate lanthanum complexes were obtained via alkane elimination utilizing the homoleptic tris(alkyl) [La{CH(SiMe₃)₂}]₃ (Scheme 6) [27,28]. The initial THF-free product is the homochiral phenolate-bridged dimer (*R,R*)-**15** (Fig. 6). Addition of THF generates the monomeric species (*R*)-**16** coordinated by three THF ligands.

Both dimeric lanthanum biphenolate complexes exhibit similar structural features for the La₂O₂-metallacycle with an unsymmetrical bridging of the phenolates (Table 4). The lanthanum to bridging phenolate bond length

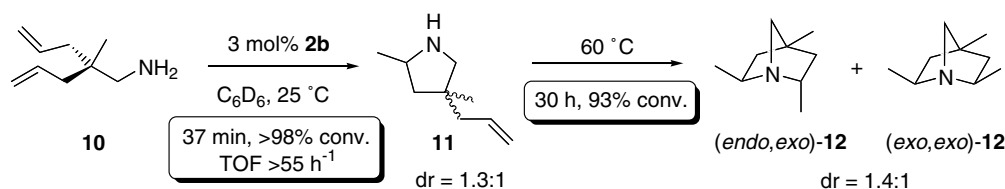
within one lanthanum-biphenolate chelate (La1–O11) is 0.10–0.14 Å longer than the La–O bond to the other lanthanum-biphenolate moiety (La1–O11'). The geometry of the biphenolate ligand is strongly dependent on the coordination number of the metal. Hence, the bite angle of the biphenolate ligand (O11–La1–O21) and the dihedral angle between the two phenolate rings is increased upon going from five coordinate (*R,S*)-**14b** to four coordinate (*R,R*)-**15**.

3.2. Asymmetric hydroamination/cyclization of aminoalkenes

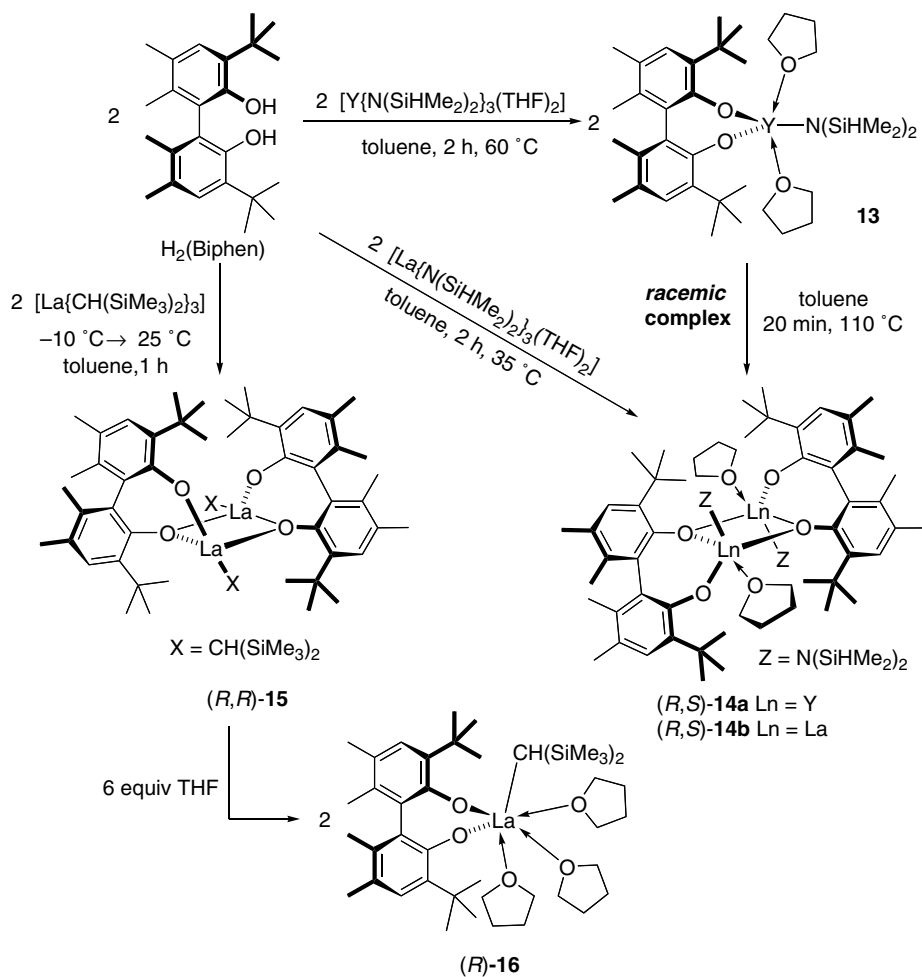
Our initial catalytic investigations revealed that the biphenolate yttrium bis(dimethylsilyl)amido complex (*R*)-**13** exhibited only low catalytic activity even at elevated temperatures (Table 5). A slight improvement in catalytic activity was observed for the binaphtholate complex (*R*)-**17**, in which the 2,6-diisopropylphenyl substituents effectively prevent formation of phenolate-bridged dimeric species. However, enantioselectivities remained moderate, reaching 57% ee for pent-4-enylamine (**6**).



Both complexes were highly thermally robust and even at 100 °C no significant loss in enantioselectivity was observed. Because intermolecular ligand redistribution reactions would lead to achiral catalytically active species, such redistribution reactions must be insignificant even under these drastic conditions and the biphenolate and binaphtholate complexes are configurational stable at least on the timescale of the catalytic reaction.



Scheme 5. Preparation of 1-aza-bicyclo[2.2.1]heptanes via bicyclization of aminodienes.



Scheme 6. Synthesis of chiral biphenolate rare earth metal complexes.

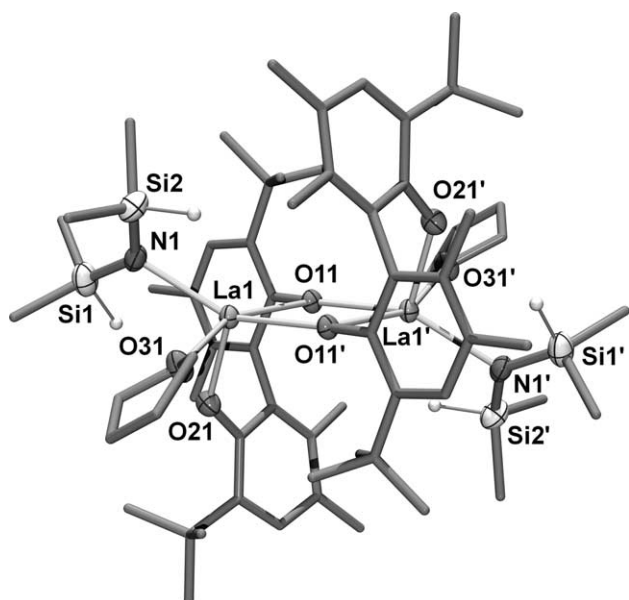


Fig. 5. Structure of heterochiral dimer (R,S)-14b.

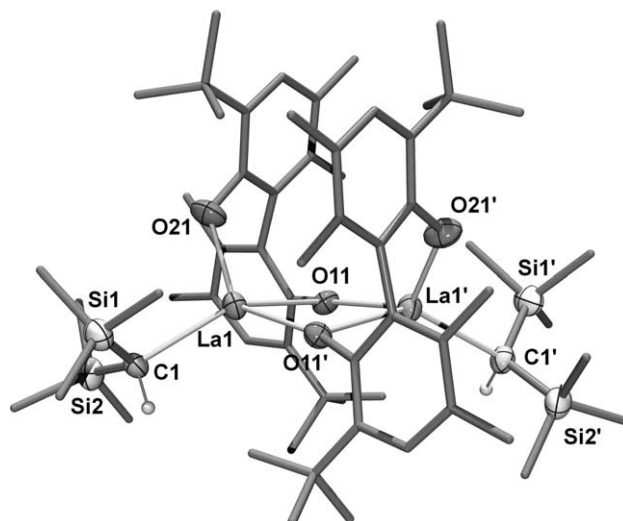


Fig. 6. Structure of homochiral dimer (R,R)-15.

Table 4

Structural comparison of selected bond lengths (Å), and angles (°) for phenolate-bridged dimers (*R,S*)-**14b** and (*R,R*)-**15**

	(<i>R,S</i>)- 14b	(<i>R,R</i>)- 15
La1–O21	2.234(2)	2.169(4)
La1–O11	2.503(2)	2.506(3)
La1–O11'	2.407(2)	2.364(3)
O11–La1–O21	88.83(7)	95.86(12)
O11–La1–O11'	71.10(8)	73.24(11)
La1–O11–La1'	108.90(8)	105.39(11)
Biphenolate dihedral angle	87.8(4)	–97.0(7)

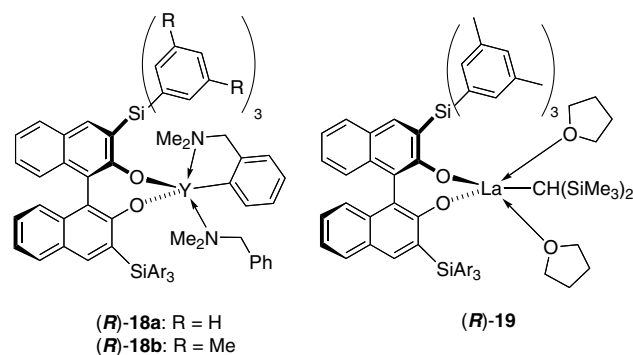
Catalysts (*R*)-**13** and (*R*)-**17** suffered from similar initiation inefficiencies and low catalytic activity as diamidoamine complex **1**, which was also indicated by their kinetic behaviour. Whereas (*R*)-**17** gave rise to a first order rate dependence on substrate concentration, (*R*)-**13** showed a second order rate dependence, contrasting the commonly observed zero order rate dependence on substrate concentration in accordance with olefin insertion into the Ln–N bond being the rate determining step [1k,6,9].

Indeed, biphenolate alkyl lanthanum complexes (*R,R*)-**15** and (*R*)-**16** displayed significant higher catalytic activity at room temperature, comparable in magnitude to lanthanocene complexes, e.g., 95 h⁻¹ for substrate **4** with [Cp₂*LaCH(SiMe₃)₂] at 25 °C [6]. The catalytic activity of the monomeric tris(THF)-adduct (*R*)-**16** was almost twice that of the homochiral dimer (*R,R*)-**15**, suggesting that the dimeric structure of the precatalyst (*R,R*)-**15** remains intact under the catalytic reaction conditions in the absence of THF. Furthermore, both catalysts showed the expected zero order rate dependence on substrate concentration.

Unfortunately, the pyrrolidine cyclization products were obtained essentially in racemic form using (*R,R*)-**15** and (*R*)-**16**, indicating that the stereodifferentiating

effect of the *tert*-butyl substituents is even less effective for the larger lanthanum in comparison to yttrium.

We concluded that a significant increase in the steric demand of the 3 and 3' substituent in the diolate ligand was necessary to improve catalyst selectivity. Indeed, binaphtholate yttrium aryl complexes (*R*)-**18a** and (*R*)-**18b** with tris(aryl)silyl substituents in 3 and 3' position performed cyclization of **4** and **6** with good rates at room temperature and better enantioselectivities compared to other biphenolate and binaphtholate complexes [30]. The highest enantioselectivities of up to 83% ee was observed for the most hindered catalyst (*R*)-**18b**. The large tris(aryl)silyl substituent did not only enhance the stereodirecting effect of the ligand, but also prevented undesired formation of phenolate-bridged dimeric species.



Addition of a few equivalents of THF diminished catalytic activity only slightly, but had a positive effect on the enantiomeric excess for substrate **4**, whereas no effect was observed for aminopentene **6** (Table 5) [31]. Obviously, in case of the sterically more demanding *gem*-dimethyl substituted aminoalkene **4**, THF can more

Table 5

Catalytic asymmetric hydroamination/cyclization of aminoalkenes

Catalyst	Substrate	[cat.]/[s] (%)	<i>T</i> (°C)	<i>t</i> (h)	Conversion (%)	TOF (h ⁻¹)	% ee
(<i>R</i>)- 13	4	4	70	22	77	2.5	36
(<i>R,R</i>)- 15	4	2	25	1.5	95	35	8
(<i>R</i>)- 16	4	2	25	1	98	61	8
(<i>R</i>)- 17	4	4	60	7	92	13.5	28.3
(<i>R</i>)- 17	4	4	100	0.75	>99		28.0
(<i>R</i>)- 18a	4	4	22	3	≥98	8	43
(<i>R</i>)- 18a + 2THF	4	1.5	25	21	≥98	6	52
(<i>R</i>)- 18b	4	4	22	2	≥98	14	53
(<i>R</i>)- 19	4	3	22	0.5	≥98	94	31
(<i>R,R</i>)- 15	6	2	60	19	>99	5	2
(<i>R</i>)- 16	6	2	60	25	98	5.3	0
(<i>R</i>)- 17	6	4	70	43	91		57
(<i>R</i>)- 17	6	4	100	16	>99		52
(<i>R</i>)- 18a	6	4	22	24	≥98	1.2	69
(<i>R</i>)- 18a + 2THF	6	1	25	54	≥98	2	67
(<i>R</i>)- 18b	6	4	22	20	≥98	2.2	83
(<i>R</i>)- 19	6	3	22	1.4	≥98	37	72

effectively compete with the substrate for empty coordination sites on the metal, changing the geometries and relative energies of the two diastereomeric cyclization transition states leading to the two enantiomeric pyrrolidine products.

Increasing the ionic radius from yttrium to lanthanum (complex (*R*)-**19**) significantly increased catalytic activity [31], although this rate improvement went along with a slight erosion in catalyst selectivity.

3.3. Kinetic resolution of chiral aminoalkenes

Asymmetric intramolecular hydroaminations are commonly performed by differentiation of enantiotopic faces of the alkene in achiral aminoalkene substrates. Chiral aminoalkenes on the other hand should be kinetically resolved, if the two enantiomers of the substrate have different rates of cyclization. That is, at 50% conversion one would obtain an enantioenriched azacyclic product and recover the aminoalkene starting material enriched with the slower reacting enantiomer.

Marks and coworkers [10c] attempted to apply chiral lanthanocene catalysts for kinetic resolution of **8**, but only low enantiomeric excess (<20% ee) at various extents of conversion was observed. Binaphtholate complexes (*R*)-**17**, (*R*)-**18a** and (*R*)-**18b** on the other hand were found to be significantly more effective in the kinetic resolution of α -substituted chiral aminopentenes (Table 6) with k_{rel} values [32] as high as 16 and enantiomeric excess for recovered starting material reaching 80% ee at conversions close to 50% [30]. The 2,5-disubstituted pyrrolidines were obtained in good to excellent *trans* diastereoselectivity, depending on the steric de-

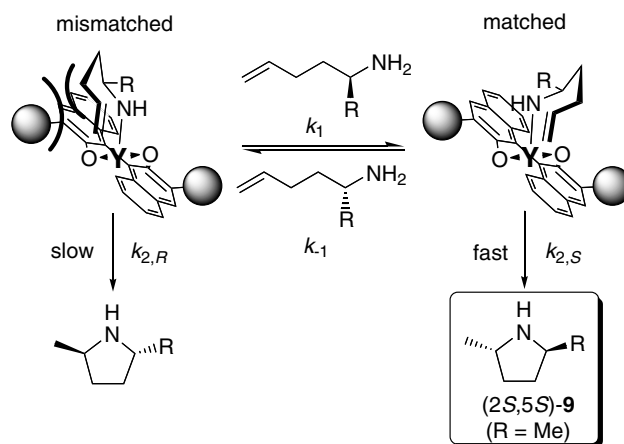
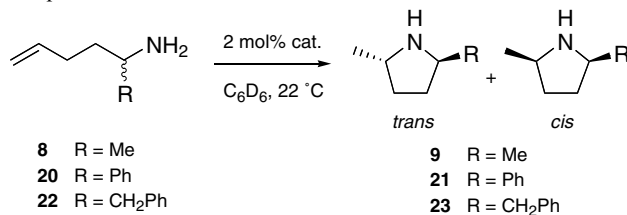


Fig. 7. Proposed stereomodel for kinetic resolution of chiral aminoalkenes with an equatorial approach of the olefin.

mand of the α -substituent. The sterically more hindered binaphtholate catalyst (*R*)-**18b** was more effective in the kinetic resolution process of the sterically less demanding **8**, whereas sterically more encumbered **20** was more efficiently kinetically resolved using (*R*)-**18a**.

A plausible stereomodel explaining the observed preferred formation of (2*S*, 5*S*)-**9** using (*R*)-**18b** as catalyst was proposed (Fig. 7). A rapid exchange of matching and mismatching aminoalkene prior to cyclization is necessary for an effective kinetic resolution process. Cyclization of (*R*)-**8** is believed to be impeded by a steric unfavorable interaction of the vinylic methylene protons with a tris(aryl)silyl substituent in the chair-like transition state. Detailed kinetic investigations are currently in progress to clarify the mechanism of this reaction.

Table 6
Catalytic kinetic resolution of chiral aminopentenes



Substrate	Catalyst	<i>t</i> (h)	Conversion (%)	<i>trans</i> : <i>cis</i>	% ee of recov. start. mat.	% ee of <i>trans</i> product (sign)	k_{rel}^a
8	(<i>R</i>)- 17 ^b	1.5	61	6.4:1	43	35	2.6
8	(<i>R</i>)- 18a	25.5	53	11:1	72	68	9.5
8	(<i>R</i>)- 18b	26	52	13:1	80	78 (–) ^c	16
20	(<i>R</i>)- 18a	95	50	≥ 50:1	74	(+)	15
20	(<i>R</i>)- 18b	18 ^d	52	≥ 50:1	63		7
22	(<i>R</i>)- 18a	9	50	20:1	42	40 (–)	3.6
22	(<i>R</i>)- 18b	27	52	20:1	38	34	2.9

^a Based on starting material.

^b 5 mol% cat., 90 °C.

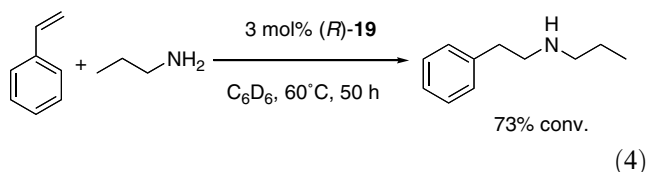
^c A (–) optical rotation corresponds to a (2*S*, 5*S*) absolute configuration.

^d At 40 °C.

3.4. Intermolecular hydroamination

The intermolecular hydroamination catalyzed by rare earth metal complexes has remained a significant challenge and efficiencies are two to three orders of magnitude smaller than for intramolecular hydroamination reactions [8]. The first order rate dependence on olefin concentration results in rather uneconomical long reaction times. Therefore, intermolecular hydroamination reactions have been commonly performed with a larger excess of olefin in order to operate in a pseudo zero order regime.

Preliminary studies have revealed recently that the highly active lanthanum catalyst (*R*)-**19** catalyzes the selective *anti*-Markovnikov addition of *n*-propylamine under relative mild reaction conditions even if only equimolar amounts of styrene and amine are used (Eq. (4)) [31], albeit rather long reaction times were required.



4. Conclusion

Non-metallocene rare earth metal complexes based on diamidoamine and diolate ligands are efficient catalysts for diastereoselective and enantioselective hydroamination reactions. They are readily prepared through convenient amine or alkane elimination procedures. The ligands are highly modular [14], allowing facile tuning of catalyst reactivity and selectivity.

The highest enantiomeric excess was achieved using sterically hindered yttrium binaphtholate complexes. These catalysts were also effective in the kinetic resolution of chiral aminoalkenes. An analogous lanthanum binaphtholate complex exhibits superior catalytic activity. It is therefore the most promising candidate for asymmetric intermolecular hydroamination reactions. Finally, current work in progress suggests that even greater enantiomeric excess in hydroamination/cyclization reactions can be achieved using rare earth elements smaller than yttrium [31].

5. Supporting information

Crystallographic data (excluding structure factors) for the structure of complex **2b** reported in this paper has been deposited with Cambridge Crystallographic Data Centre as supplementary publication no. CCDC-

251073. Copies of the data can be obtained free of charge from the Director, CCDC, 12 Union Road, Cambridge CB2 1EZ, UK; fax: (int code) +44 1223/336 033 or E-mail: deposit@ccdc.cam.ac.uk or www: <http://www.ccdc.cam.ac.uk>.

Acknowledgement

Generous financial support by the Deutsche Forschungsgemeinschaft (DFG) and the Fonds der Chemischen Industrie is gratefully acknowledged. K.C.H. is a DFG Emmy Noether fellow (2001–2005) and thanks Professor John A. Gladysz for his generous support.

References

- [1] (a) R. Taube, in: B. Cornils, W.A. Herrmann (Eds.), Applied Homogeneous Catalysis, vol. 1, Wiley-VCH, Weinheim, 1996, pp. 507–526;
- (b) T.E. Müller, M. Beller, Chem. Rev. 98 (1998) 675–703;
- (c) T.E. Müller, M. Beller, in: M. Beller, C. Bolm (Eds.), Transition metals for organic synthesis, vol. 2, Wiley-VCH, Weinheim, 1998, pp. 316–330;
- (d) M. Nobis, B. Drieffen-Hölscher, Angew. Chem. Int. Ed. 40 (2001) 3983–3985;
- (e) J.J. Brunet, D. Neibecker, in: A. Togni, H. Grützmacher (Eds.), Catalytic heterofunctionalization from hydroamination to hydrozirconation, Wiley-VCH, Weinheim, 2001, pp. 91–141;
- (f) J. Seayad, A. Tillack, C.G. Hartung, M. Beller, Adv. Synth. Catal. 344 (2002) 795–813;
- (g) M. Beller, C. Breindl, M. Eichberger, C.G. Hartung, J. Seayad, O.R. Thiel, A. Tillack, H. Trauthwein, Synlett (2002) 1579–1594;
- (h) F. Pohlki, S. Doye, Chem. Soc. Rev. 32 (2003) 104–114;
- (i) I. Bytschkov, S. Doye, Eur. J. Org. Chem. (2003) 935–946;
- (j) S. Doye, Synlett (2004) 1653–1672;
- (k) S. Hong, T.J. Marks, Acc. Chem. Res. 37 (2004) 673–686.
- [2] (a) P.W. Roesky, T.E. Müller, Angew. Chem. Int. Ed. 42 (2003) 2708–2710;
- (b) K.C. Hultsch, Adv. Synth. Catal. 347 (2005) 367–391.
- [3] (a) For some recent example of asymmetric hydroamination using group 4 metal complexes see: P.D. Knight, I. Munslow, P.N. O'Shaughnessy, P. Scott, Chem. Commun. (2004) 894–895;
- (b) J.M. Hoover, J.R. Petersen, J.H. Pikul, A.R. Johnson, Organometallics 23 (2004) 4614–4620.
- [4] (a) For some recent example of asymmetric hydroamination using late transition metal complexes see: R. Dorta, P. Egli, F. Zürcher, A. Togni, J. Am. Chem. Soc. 119 (1997) 10857–10858;
- (b) M. Kawatsura, J.F. Hartwig, J. Am. Chem. Soc. 122 (2000) 9546–9547;
- (c) O. Löber, M. Kawatsura, J.F. Hartwig, J. Am. Chem. Soc. 123 (2001) 4366–4367;
- (d) W. Zhuang, R.G. Hazell, K.A. Jørgensen, Chem. Commun. (2001) 1240–1241;
- (e) L. Fadini, A. Togni, Chem. Commun. (2003) 30–31;
- (f) K. Li, K.K. Hii, Chem. Commun. (2003) 1132–1133;
- (g) K. Li, P.N. Horton, M.B. Hursthouse, K.K. Hii, J. Organomet. Chem. 665 (2003) 250–257;
- (h) L.M. Lutete, I. Kadota, Y. Yamamoto, J. Am. Chem. Soc. 126 (2004) 1622–1623;
- (i) K. Li, X. Cheng, K.K. Hii, Eur. J. Org. Chem. (2004) 959–964.

- [5] (a) Furthermore, alkali metals and mercury salts have been applied as reagents or catalysts for hydroamination, respectively, aminomercuration, see for example: R. Wegler, G. Pieper, *Chem. Ber.* 83 (1950) 1–6;
 (b) R.J. Schlott, J.C. Falk, K.W. Narducy, *J. Org. Chem.* 37 (1972) 4243–4245;
 (c) G.P. Pez, J.E. Galle, *Pure Appl. Chem.* 57 (1985) 1917–1926;
 (d) C. Koradin, W. Dohle, A.L. Rodriguez, B. Schmid, P. Knochel, *Tetrahedron* 59 (2003) 1571–1587;
 (e) For reviews see Ref. [1e,1f], see also: R.C. Larock, W.M. Leong, in: B.M. Trost, I. Fleming (Eds.), *Comprehensive Organic Synthesis*, vol. 4, Pergamon Press, Oxford, 1991, pp. 290–295.
- [6] M.R. Gagné, C.L. Stern, T.J. Marks, *J. Am. Chem. Soc.* 114 (1992) 275–294.
- [7] (a) For a more general review on the application of organo rare earth metal catalysts in organic synthesis see: G.A. Molander, E.D. Dowdy, *Top. Organomet. Chem.* 2 (1999) 119–154;
 (b) G.A. Molander, J.A.C. Romero, *Chem. Rev.* 102 (2002) 2161–2185.
- [8] (a) Y. Li, T.J. Marks, *Organometallics* 15 (1996) 3770–3772;
 (b) J.-S. Ryu, G.Y. Li, T.J. Marks, *J. Am. Chem. Soc.* 125 (2003) 12584–12605.
- [9] A. Motta, G. Lanza, I.L. Fragalà, T.J. Marks, *Organometallics* 23 (2004) 4097–4104.
- [10] (a) M.R. Gagné, L. Brard, V.P. Conticello, M.A. Giardello, T.J. Marks, C.L. Stern, *Organometallics* 11 (1992) 2003–2005;
 (b) M.A. Giardello, V.P. Conticello, L. Brard, M. Sabat, A.L. Rheingold, C.L. Stern, T.J. Marks, *J. Am. Chem. Soc.* 116 (1994) 10212–10240;
 (c) M.A. Giardello, V.P. Conticello, L. Brard, M. Gagné, T.J. Marks, *J. Am. Chem. Soc.* 116 (1994) 10241–10254.
- [11] (a) Epimerization of planar chiral cyclopentadienyl rare earth metal complexes has also been observed in the presence of donor solvents, such as ether or THF, see: C.M. Haar, C.L. Stern, T.J. Marks, *Organometallics* 15 (1996) 1765–1784;
 (b) K.C. Hultsch, T.P. Spaniol, J. Okuda, *Organometallics* 16 (1997) 4845–4856;
 (c) J.C. Yoder, M.W. Day, J.E. Bercaw, *Organometallics* 17 (1998) 4946–4958;
 (d) J. Eppinger, Ph.D. Thesis, Technische Universität München 1999.
- [12] (a) M.R. Douglass, M. Ogasawara, S. Hong, M.V. Metz, T.J. Marks, *Organometallics* 21 (2002) 283–292;
 (b) J.-S. Ryu, T.J. Marks, F.E. McDonald, *J. Org. Chem.* 69 (2004) 1038–1052;
 (c) S. Hong, A.M. Kawaoka, T.J. Marks, *J. Am. Chem. Soc.* 125 (2003) 15878–15892.
- [13] (a) For general reviews on the chemistry of cyclopentadienyl-free rare earth metal complexes see: F.T. Edelman, *Angew. Chem. Int. Ed.* 34 (1995) 2466–2488;
 (b) F.T. Edelman, D.M.M. Freckmann, H. Schumann, *Chem. Rev.* 102 (2002) 1851–1896;
 (c) W.E. Piers, D.J.H. Emslie, *Coord. Chem. Rev.* 233–234 (2002) 131–155.
- [14] (a) Even simple modifications to the ligand structure of cyclopentadienyl ligands can require tedious multistep procedures, see for example: R.L. Halterman, *Chem. Rev.* 92 (1992) 965–994;
 (b) R.L. Halterman, in: A. Togni, R.L. Halterman (Eds.), *Metallocenes*, vol. 1, Wiley-VCH, Weinheim, 1998, pp. 455–544.
- [15] (a) M.R. Bürgstein, H. Berberich, P.W. Roesky, *Organometallics* 17 (1998) 1452–1454;
 (b) M.R. Bürgstein, H. Berberich, P.W. Roesky, *Chem. Eur. J.* 7 (2001) 3078–3085;
 (c) Y.K. Kim, T. Livinghouse, J.E. Bercaw, *Tetrahedron Lett.* 42 (2001) 2933–2935.
- [16] (a) Y.K. Kim, T. Livinghouse, *Angew. Chem. Int. Ed.* 41 (2002) 3645–3647;
 (b) Y.K. Kim, T. Livinghouse, Y. Horino, *J. Am. Chem. Soc.* 125 (2003) 9560–9561.
- [17] (a) P.N. O’Shaughnessy, P. Scott, *Tetrahedron Asymmetry* 14 (2003) 1979–1983;
 (b) P.N. O’Shaughnessy, P.D. Knight, C. Morton, K.M. Gillespie, P. Scott, *Chem. Commun.* (2003) 1770–1771;
 (c) S. Hong, S. Tian, M.V. Metz, T.J. Marks, *J. Am. Chem. Soc.* 125 (2003) 14768–14783;
 (d) J. Collin, J.-D. Daran, E. Schulz, A. Trifonov, *Chem. Commun.* (2003) 3048–3049;
 (e) P.N. O’Shaughnessy, K.M. Gillespie, P.D. Knight, I. Munslow, P. Scott, *J. Chem. Soc. Dalton Trans.* (2004) 2251–2256.
- [18] (a) R.R. Schrock, A.L. Casado, J.T. Goodman, L.-C. Liang, P.J.J. Bonitatebus Jr., W.M. Davis, *Organometallics* 19 (2000) 5325–5341;
 (b) R.R. Schrock, P.J.J. Bonitatebus Jr., Y. Schrodi, *Organometallics* 20 (2001) 1056–1058;
 (c) Y. Schrodi, R.R. Schrock, P.J.J. Bonitatebus Jr., *Organometallics* 20 (2001) 3560–3573.
- [19] K.C. Hultsch, F. Hampel, T. Wagner, *Organometallics* 23 (2004) 2601–2612.
- [20] (a) Crystal structure analysis of **2b**: Clear, colourless crystals of **2b** suitable for X-ray diffraction analysis were obtained by cooling of a concentrated pentane solution to $-30\text{ }^{\circ}\text{C}$. Data were collected on a Nonius KappaCCD area detector. Crystal data for **2b**: $\text{C}_{31}\text{H}_{55}\text{N}_4\text{Si}_2\text{Y}$, $M_r = 628.88$, crystal size $0.20 \times 0.15 \times 0.10$ mm, orthorhombic, space group $\text{Pna}2_1$ (racemic twin), $a = 17.6341(3)$ Å, $b = 17.9796(6)$ Å, $c = 11.1808(4)$ Å, $V = 3544.92(18)$ Å³, $Z = 4$, $\rho_{\text{calcd}} = 1.178$ g cm⁻³, $F(000) = 1344$, Mo- K_{α} radiation ($\lambda = 0.71073$ Å), $T = 173(2)$ K, $\mu = 1.736$ mm⁻¹, 7853 independent reflections measured, $\text{GOF} = 1.027$, $R(I > 2\sigma(I)) = 0.0491$, $wR_2(\text{all data}) = 0.1257$, absolute structure parameter = $0.495(7)$, largest e -max, e -min = 0.409 and -0.374 e Å⁻³. Cell parameters for **2b** were obtained from 10 frames using a 10° scan and refined with 4441 reflections. Lorentz, polarization, and empirical absorption corrections were applied [20b,20c]. The space group was determined from systematic absences and subsequent least-squares refinement. The structures were solved by direct methods. The parameters were refined with all data by full-matrix-least-squares on F^2 using SHELXL-97 [20d]. Hydrogen atoms were fixed in idealized positions using a riding model. Non-hydrogen atoms were refined anisotropically. Scattering factors, and $\Delta f'$ and $\Delta f''$ values, were taken from literature [20e];
 (b) “Collect” data collection software, Nonius B.V. 1998;
 (c) Z. Otwinowski, W. Minor, “Scalepack” data processing software, Meth. Enzymol (Macromol. Crystallogr. Part A) 276 (1997) 307;
 (d) G.M. Sheldrick, SHELX-97, Program for the refinement of crystal structures, University of Göttingen, 1997;
 (e) D.T. Cromer, J.T. Waber, in: J.A. Ibers, W.C. Hamilton (Eds.), *International Tables for X-ray Crystallography*, Kynoch, Birmingham, England, 1974.
- [21] (a) K.H. den Haan, J.L. de Boer, J.H. Teuben, A.L. Spek, B. Kojic-Prodic, G.R. Hays, R. Huis, *Organometallics* 5 (1986) 1726–1733;
 (b) M. Westerhausen, M. Hartmann, A. Pfitzner, W. Schwarz, *Z. Anorg. Allg. Chem.* 621 (1995) 837–850;
 (c) Y. Mu, W.E. Piers, M.-A. MacDonald, M.J. Zaworotko, *Can. J. Chem.* 73 (1995) 2233–2238;
 (d) M.H. Lee, J.-W. Hwang, Y. Kim, J. Kim, Y. Han, Y. Do, *Organometallics* 18 (1999) 5124–5129, see also Ref. [10b].
- [22] (a) $pK_a(\text{HN}(\text{SiHMe}_2)_2) = 22.8$, see: J. Eppinger, M. Spiegler, W. Hieringer, W.A. Herrmann, R. Anwander, *J. Am. Chem. Soc.* 122 (2000) 3080–3096;
 (b) $pK_a(\text{HN}(\text{SiMe}_3)_2) = 25.8$, see: R.R. Fraser, T.S. Mansour, S. Savard, *J. Org. Chem.* 50 (1985) 3232–3234.

- [23] E.L. Eliel, S.H. Wilen, *Stereochemistry of Organic Compounds*, Wiley, 1994.
- [24] J.-S. Ryu, T.J. Marks, F.E. McDonald, *Org. Lett.* 3 (2001) 3091–3094.
- [25] Except for the crystal structure analysis of a less active and less selective bis(thiophosphinic amidate) complex (see Ref. [16b]), no NMR spectroscopic evidence or any other analytical data to proof the claimed catalyst composition has been disclosed.
- [26] D.V. Gribkov, K.C. Hultzsch, F. Hampel, *Chem. Eur. J.* 9 (2003) 4796–4810.
- [27] D.V. Gribkov, F. Hampel, K.C. Hultzsch, *Eur. J. Inorg. Chem.* (2004) 4091–4101.
- [28] Schaverien, et al. reported the synthesis of related racemic biphenolate and binaphtholate complexes, see: C.J. Schaverien, N. Meijboom, A.G. Orpen, *J. Chem. Soc. Chem. Commun.* (1992) 124–126.
- [29] These biphenolate ligands have been successfully applied in asymmetric ring-closing metathesis catalysts, see: R.R. Schrock, A.H. Hoveyda, *Angew. Chem. Int. Ed.* 42 (2003) 4592–4633.
- [30] D.V. Gribkov, K.C. Hultzsch, *Chem. Commun.* (2004) 730–731.
- [31] D.V. Gribkov, K.C. Hultzsch, unpublished results.
- [32] k_{rel} denotes the relative ratio between the faster and slower reacting enantiomer of the substrate, see: H.B. Kagan, J.C. Fiaud, *Top. Stereochem.* 18 (1988) 249–330.